

## EXAFS analysis using *FEFF* and *FEFFIT*

Matthew Newville

Consortium for Advanced Radiation Sources, The University of Chicago, 5640 South Ellis Avenue, Chicago, IL 60637, USA.  
E-mail: newville@cars.uchicago.edu

Some of the advanced EXAFS analysis features of *FEFF* and *FEFFIT* are described. The scattering path formalism from *FEFF* and cumulant expansion are used as the basic building blocks of EXAFS analysis, giving a flexible and robust parameterization of most EXAFS problems. The ability to model EXAFS data in terms of generalized physical variables is shown, including the simultaneous refinement of two different polarizations for Co K EXAFS data of CoPt<sub>3</sub>.

**Keywords:** XAFS; *FEFF*; *FEFFIT*.

### 1. Introduction

The use of *ab initio* calculations of scattering phase shifts and amplitudes for EXAFS analysis has become standard practice in the past decade. Though scattering phase shifts and amplitudes derived from experiment or tables (McKale *et al.*, 1988) are still in use, *ab initio* calculations from the programs *EXCURVE* (Binsted *et al.*, 1991, 1992; Binsted & Hasnain, 1996), *GNXAS* (Filippini *et al.*, 1995) and especially *FEFF* (Zabinsky *et al.*, 1995) have come to dominate the field. In the proceedings of the XAFS X conference (Hasnain *et al.*, 1999), for example, of the quantitative EXAFS analyses† presented, more used *FEFF* than all other methods combined. Use of experimental and tabulated standards were each below 10%, and use of the *ab initio* codes *EXCURVE* and *GNXAS* were each below 15%.

These statistics reflect a change in the field that is unlikely to be reversed soon. To understand and use XAFS at this time, one must come to understand *FEFF*, its strengths and its limitations. This is not to imply that using *FEFF* is always the best way to analyze XAFS data, or that having one theoretical program dominating the field is necessarily good. Still, even if one does not use *FEFF*, one must understand the physical approximations implemented in the code well enough to assess results based on it.

The widespread use of *FEFF* may be related to it being *only* a theoretical code, with no analysis program included as part of an integrated package, as both *EXCURVE* and *GNXAS* provide. Instead, many analysis programs (George & Pickering, 1995; Bouldin *et al.*, 1995; Michalowicz, 1995; Vaarkamp *et al.*, 1994; Ressler, 1997; Newville *et al.*, 1995) can use the results of *FEFF*. This separation of *ab initio* theory from analysis allows quite a bit of flexibility, but puts more burden of understanding the calculation details on the user, or at the least authors of analysis programs.

While the theoretical understanding of X-ray absorption that leads to reliable and efficient computation of the XAFS phase shifts and amplitudes from *FEFF* is well documented (Rehr & Ankudinov, 2001; Rehr & Albers, 2000), comparatively little has been published about the use of *FEFF* for EXAFS analysis. One early study (O'Day *et al.*, 1994) is notable for its demonstration of the suitability of *FEFF*

† That is, analyses in which numerical results were derived from  $\chi(k)$ . Theoretical papers and XANES analyses were not included. 109 of the 242 papers in the proceedings met these criteria. Of these, 70 used *FEFF*, 15 *EXCURVE*, 7 *GNXAS*, 8 McKale *et al.* (1988) and 9 experimental or unspecified standards.

in analyzing real EXAFS data. Comparisons of theoretical phase shifts from different calculations have been made (Vaarkamp *et al.*, 1994; Vaarkamp, 1993), but are rare. Some comparisons of different potential models within *FEFF* have been made (Bridges & Rehr, 1998), but are largely anecdotal.

In this paper, I will describe some of the practical aspects of using *FEFF* for EXAFS analysis. The emphasis here is not on the physics underlying the calculations performed by *FEFF*, but on how these results are applied to analyzing EXAFS data. Though *FEFF* is in constant development, version 7.02 will be used in this work. I will also describe the EXAFS analysis program *FEFFIT* (Newville *et al.*, 1995), which extends the utility of *FEFF* and adds the ability to parameterize and fit XAFS data to *FEFF* calculations. Special attention will be placed on the advanced modeling capabilities of *FEFFIT*, including the use of 'generalized fitting parameters' and the simultaneous refinement of multiple data sets.

### 2. The outputs of *FEFF*

As an *ab initio* calculation, *FEFF* uses a list of atomic coordinates in a cluster and physical information about the system such as absorbing atom and excited core-level for its calculation. For crystalline systems, generating a list of atomic coordinates is simplified by the program *ATOMS* (Ravel, 2001) which generates the required coordinates (as well as reasonable defaults for most *FEFF* parameters) starting from a crystallographic description of the system.

*FEFF* (versions 5 through 7) calculates EXAFS using four internal modules: *POTPH*, *PATHS*, *GENFMT* and *FF2CHI*. *POTPH* creates atomic potentials based on the geometrical distribution of atoms, overlaps their wavefunctions, and calculates the scattering phase-shifts based on these potentials. Electronic models including exchange energies and inelastic processes are used, and much of the fundamental research and published literature on *FEFF* is devoted to these parts of the calculation (Rehr *et al.*, 1986, 1991, 1992; Ankudinov & Rehr, 1995; Ankudinov, Conradson *et al.*, 1998). For the purposes here, *POTPH* generates the file *phase.bin*, which is unreadable by humans, but used in later parts of the calculation. For better XANES calculations, *FEFF8* (Ankudinov, Ravel *et al.*, 1998) breaks *POTPH* into three modules, but the outcome for EXAFS analysis is still *phase.bin*.

The *PATHS* module (Zabinsky *et al.*, 1995) identifies all single- and multiple-scattering paths for an arbitrary cluster of atoms. Many candidate scattering paths are efficiently rejected at this stage on the basis of a quick estimate of the scattering amplitude. In addition, degenerate paths that will give identical XAFS contributions are recognized at this stage, resulting in a handful of scattering paths that dominate the EXAFS even out to the fourth-neighbor distance in well ordered systems. The geometries of the unique paths are written to the file *paths.dat*, sorted by distance from the absorbing atom. This file can be very helpful in identifying and describing the path geometries.

The *GENFMT* module (Rehr & Albers, 1990) uses the results of *POTPH* (*phase.bin*) and *PATHS* (*files.dat*) to calculate the XAFS contribution from each path. Though the full complex fine-structure  $\tilde{\chi}(k)$  is calculated directly for each path from the potentials and scattering phase shifts, the results are broken down at this stage so as to be described by a simplified version of the familiar EXAFS equation for each path *j*,

$$\tilde{\chi}_j(k) = \frac{N_j F_j(k) \exp[-2R_j/\lambda(k)]}{kR_j^2} \exp[i2kR_j + i\delta_j(k)]. \quad (1)$$

Here,  $N_j$  is the number of equivalent paths,  $F_j(k)$  is the effective scattering amplitude,  $\delta_j(k)$  is the effective total phase shift (including contributions from the central atom and all scattering atoms), and  $R_j$  is half the total length of the scattering path. In principle, both  $F_i$  and  $\delta_i$  will have some dependence on the distance between atoms, but any  $R$  dependence of these terms is left out of this simple expression. No thermal or configurational disorder is included at this point.

In equation (1),  $k$  is the wavenumber and  $\lambda(k)$  is the mean free path of the photoelectron. These both depend on the details of the potentials for the cluster, but are independent of scattering path. The EXAFS contribution for each path is written to the file *FEFFnnnn.dat*, where *nnnn* is replaced by the path index  $j$ . The file *list.dat* (or *files.dat* in earlier versions of *FEFF*) gives a simple list of the *feffnnnn.dat* files including  $R_j$  and the number of legs in the path.

*FF2CHI*, the final module of *FEFF*, performs the relatively simple sum over paths  $j$  to generate the complex  $\tilde{\chi}(k)$ ,

$$\tilde{\chi}(k) = \sum_j \tilde{\chi}_j(k) \exp(-2k^2\sigma_j^2), \quad (2)$$

which can be compared with experimental  $\chi(k)$  by taking the imaginary part. Here, disorder can be added through a Debye–Waller factor to give the EXAFS a realistic decay. Values for  $\sigma_j^2$  can be given explicitly, or calculated using a Debye or Einstein model. The results are written to the file *chi.dat*, which contains arrays for  $k$ ,  $\text{Im}[\tilde{\chi}(k)]$ ,  $|\chi(k)|$  and the phase of  $\tilde{\chi}(k)$ .

### 2.1. The structure of *feffnnnn.dat*

For EXAFS analysis, either the full *chi.dat* or the individual *feffnnnn.dat* files can be used. Many analysis programs use the *chi.dat* as this resembles experimentally derived standards for EXAFS. Though convenient, this is not a very flexible approach, and is not well suited to including the effects of large disorder. The preferred method is to use the *feffnnnn.dat* files. The structure of these files, shown in Fig. 1, is somewhat complex. In order to recover the variables in equation (1) from the data in this file, the mapping shown in Table 1 is used. The  $k$ -dependent arrays in *feffnnnn.dat* are given on a coarser grid than is typically used for XAFS, but are smooth enough functions of  $k$  that linear interpolation can be used. In addition to the variables in equation (1), the *complex* photoelectron wavenumber,  $p(k)$ , is also defined here, and will be used below to modify (1).  $k$  is purely real, relative to the onset of absorption at the Fermi level, and

```

Cobalt Platinum                               Feff 7.023
CoPt3
Abs Z=27 Rmt= 1.347 Rnm= 1.463 K shell
Pot 1 Z=27 Rmt= 1.352 Rnm= 1.470
Pot 2 Z=78 Rmt= 1.356 Rnm= 1.481
Gam_ch=1.457E+00 H-L exch
Mu=-3.459E+00 kf=1.968E+00 Vint=-1.822E+01 Rs_int= 1.843
Path 1 icalc 2
-----
2 1.000 2.7089 2.7944 -3.45884 nleg, deg, reff, rnmav(bohr), edge
x y z pot at#
0.0000 0.0000 0.0000 0 27 Co absorbing atom
1.9155 -1.9155 0.0000 1 27 Co
k real[2*phc] mag[feff] phase[feff] red factor lambda real[p]#
0.000 2.1669E+00 0.0000E+00 -3.1308E+00 1.040E+00 2.0596E+01 1.9689E+00
0.100 2.1649E+00 4.4413E-02 -3.6603E+00 1.039E+00 2.0621E+01 1.9713E+00
0.200 2.1591E+00 8.8080E-02 -4.1653E+00 1.039E+00 2.0694E+01 1.9786E+00
0.300 2.1494E+00 1.3031E-01 -4.6458E+00 1.039E+00 2.0809E+01 1.9907E+00
0.400 2.1358E+00 1.7052E-01 -5.1023E+00 1.039E+00 2.0953E+01 2.0075E+00
0.500 2.1185E+00 2.0824E-01 -5.5348E+00 1.039E+00 2.1111E+01 2.0289E+00
    
```

Figure 1

Sample *feffnnnn.dat*: *feff0001.dat* for first-neighbor Co–Co scattering in CoPt<sub>3</sub>. After a series of comment lines ending with the line -----, the number of legs, number of equivalent paths, half path-length  $R_j$  (2.7089 Å here), Norman radius and Fermi energy relative to  $E_0$  are given, followed by coordinates of the atoms in the path, and then a list of  $k$ -dependent arrays (truncated here) used to reconstruct  $\tilde{\chi}_j(k)$ .

Table 1

Correspondence of the variables in equation (1) to the entries of a *feffnnnn.dat* file.

Variable	Value from <i>feffnnnn.dat</i>
$R_j$	reff
$N_j$	deg
$k$	k
$F_j(k)$	mag[feff] * 'red factor'
$\delta_j(k)$	real[2*phc] + phase[feff]
$\lambda(k)$	lambda
$p(k)$	real[p] + i/lambda

so is comparable with the experimentally determined  $k$ . It is used to reconstruct  $\tilde{\chi}(k)$  as calculated by *FEFF*.  $p$  is complex (the imaginary part representing losses of photoelectron coherence including the mean free path and core-hole lifetime), relative to the continuum level  $E_0$ , and the more appropriate measure of photoelectron momentum to use for the modification of equation (1).

### 2.2. Polarization dependence in *FEFF*

*FEFF* can accurately calculate the polarization dependence of EXAFS, as well as related techniques such as X-ray magnetic circular dichroism (Ankudinov & Rehr, 1997). For  $K$ -edge calculations at sufficiently high  $k$ , the usual  $\cos^2(\alpha)$  dependence (Stern, 1988) of the angle  $\alpha$  between scattering path and polarization directions works very well. Using *FEFF*'s polarized calculations for  $K$ -edge EXAFS is not much of an improvement over simply multiplying the unpolarized calculation by  $\cos^2(\alpha)/3$ . The factor of three can lead to some confusion, as *FEFF* will always report the full coordination shell, even though some of the atoms do not contribute.† The polarization of  $L_{II}$  and  $L_{III}$  edges is somewhat more complex (Stern, 1988; Rehr & Albers, 2000), including isotropic as well as a  $\cos^2(\alpha)$  term. The relative sizes of these terms depends on the scattering matrix elements and whether the  $p \rightarrow s$  transitions are included (Ankudinov & Rehr, 1997).

### 3. The structure of *FEFFIT*

*FEFFIT* essentially replaces the *FF2CHI* module of *FEFF*, expanding the EXAFS equation (1) and enhancing the sum over paths of equation (2) using a set of *feffnnnn.dat* files. Even in the simplest respect of forward-modeling XAFS spectra, *FEFFIT* has several advantages over the *FF2CHI* module of *FEFF*, including the ability to combine calculations from different *FEFF* runs (as for different central-atom locations in systems with multiple sites), and the ability to Fourier transform theoretical spectra (both total and individual paths, and with and without 'phase corrections') into  $\chi(R)$ .

Since the *feffnnnn.dat* files represent the EXAFS from a path with exact atomic coordinates, any thermal or configurational disorder must be added at this stage. Indeed, information about the partial pair distribution function  $g(R)$  of atoms around the absorbing atom is often the goal of EXAFS analysis. *FEFFIT* uses the cumulant expansion (Bunker, 1983; Kendall, 1958) which is independent of any model for  $g(R)$  and converges with a small number of cumulants for small and moderate disorders. The first four cumulants ( $\Delta R$ ,  $\sigma^2$ ,  $C_3$  and  $C_4$ ) of the distribution  $g(R)$  can be determined with *FEFFIT*, though  $C_4$  is rarely important.

There are two subtle but important points to be considered when using the cumulant expansion in systems with large disorder. First,

† In a simple cubic material,  $K$ -edge EXAFS with the polarization vector along (100) would only be sensitive to two near-neighbor atoms. *FEFF* will report that six neighbors contribute.

the  $1/kR^2$  dependence of  $\chi(k)$  must be included. This can be performed simply and accurately (Tranquada & Ingalls, 1983) by adding a term of the form  $-2k\sigma^2/R$  to  $\Delta R$ . The second point is specific to using *ab initio* calculations from which losses can be described in terms of a mean free path: the complex  $p$  should be used instead of  $k$  to model the disorder. This mixes the phase and amplitude effects of each of the cumulants, which can be important for large disorder. The resulting modified EXAFS equation is

$$\begin{aligned} \tilde{\chi}_j(k) = & \frac{S_{0j}^2 N_j F_j(k)}{k(\Delta R_j + R_j)^2} \exp\{i[2kR_j + \delta_j(k)]\} \\ & \times \exp[i(2p\Delta R_j - 4p\sigma_j^2/R_j - 4p^3 C_{3j}/3)] \\ & \times \exp[-2R_j/\lambda(k) - 2p^2\sigma_j^2 - 2p^4 C_{4j}/3]. \end{aligned} \quad (3)$$

As noted above, both  $k$  and  $p$  are used here. Although  $p$  is used to modify the EXAFS based on the cumulants, we must first reconstruct  $\tilde{\chi}_j(k)$  from the *feffnnnn.dat* files according to equation (1). In addition to the four cumulants, values for a constant amplitude factor  $S_{0j}^2$ , an energy shift  $E_0$  which will modify the values of  $k$  used, and a broadening energy term  $E_i$  which will modify  $\lambda(k)$ , can be modified for each path  $j$ . Thus, up to seven path parameters can be used to modify the EXAFS contribution for each path.

### 3.1. Path parameters and generalized variables

Though useful for modeling, the seven independent path parameters available in *FEFFIT* for each scattering path are more than can usually be determined from real EXAFS data. The limited amount of information available from EXAFS data can be described using the number of independent parameters that can be obtained from a periodic signal (Lytle *et al.*, 1989; Brillouin, 1962)

$$N_{\text{info}} \simeq 2\Delta k \Delta R/\pi, \quad (4)$$

where  $\Delta k$  and  $\Delta R$  are the extent of the data in  $k$ - and  $R$ -space under consideration, respectively.†

The approximate nature of equation (4) should be emphasized, especially as noise in the data is not considered here. The suggestion (Stern, 1993) that *more* parameters can be determined than is given by (4) has not proven particularly beneficial. More sophisticated statistical treatments (Curis & Benazeth, 2000) may be helpful for assessing how many and what parameters can be obtained from EXAFS data, but have proven difficult to implement for general analysis of individual spectra. Methods explicitly taking the entropy of the spectra into account (Krappe & Rossner, 2000) may also prove useful in quantifying the number of parameters that can be obtained from a given spectra, and have the potential of being able to take noise into account.

Because of the limited information in EXAFS, it is not meaningful to adjust all seven path parameters independently, especially when scattering paths involving different neighboring atoms overlap in a 'shell'. Many parameters (notably  $E_p$ ,  $C_4$  and often  $C_3$ ) will not need adjustment at all. In addition, several parameters for different paths may take the same value or values that are simply related. Therefore, a system with constraints and algebraic relations between the parameters of a single path, different paths or even different sets of data is desirable. *FEFFIT* allows the path parameters for each path to be written as algebraic expressions of a set of 'generalized variables',

† It is occasionally thought that this limitation is due to the Fourier transform performed during analysis, and that by analyzing data in  $E$ - or  $k$ -space this limitation can be avoided. This notion is wrong. The limitation is due to the finite extent of  $g(R)$  for a given shell, not the data processing methods. A measurement of  $\mu(E)$  may contain 400 independent measurements of  $\mu(E)$ , but it does not give 400 independent samples of the first-neighbor distance.

which can be varied to fit a set of data. The effect of the generalized variables on the path parameters can be quite complex, but a simple example would be to use one  $E_0$  and one  $S_0^2$  parameter for all paths in a fit. Such a constraint is not necessarily *required*, but commonly used.

*FEFFIT*'s system of generalized variables and user-defined expressions for path parameters gives a wide range of possible constraint equations, allows physically meaningful sets of variables to be fit directly from XAFS data, and helps to limit the number of free parameters in a fit. Several examples (Frenkel *et al.*, 1994; Ravel *et al.*, 1999; Kelly *et al.*, 1998) have used *FEFFIT*'s advanced modeling capabilities. Many of these examples rely on the important ability of *FEFFIT* to simultaneously refine multiple sets of data. A simple example will be given in §4.

### 3.2. Approaches to fitting and error analysis

*FEFFIT* combines and modifies the EXAFS from a set of *feffnnnn.dat* files to best-fit experimental  $\chi(k)$  data. Recently, *FEFFIT* has also been used with experimental standards as described elsewhere in these proceedings (Frenkel *et al.*, 2001). The fit can be performed on data in  $k$ -,  $R$ - or back-transformed  $k$ -space. In general, fitting in  $R$ -space gives the most satisfactory results, the most control over what portion of the spectra is studied, and the most meaningful error analysis. The fitting is performed with the Levenberg-Marquardt (Marquardt, 1963) method of non-linear least-squares minimization. Given the set of  $P$  generalized variables  $\mathbf{x}$ , the most likely values  $\mathbf{x}_0$  are those found to minimize

$$\chi^2 = \frac{N_{\text{info}}}{N} \sum_{i=i'}^{N+i'-1} \left[ \frac{\tilde{\chi}_{\text{data}}(R_i) - \tilde{\chi}_{\text{model}}(R_i, \mathbf{x})}{\varepsilon_i} \right]^2 \quad (5)$$

where  $\tilde{\chi}(R)$  represents the real and imaginary components of the Fourier transform of  $\chi(k)$  and  $\varepsilon$  is the estimated uncertainty of the data (Newville *et al.*, 1999). The sum for  $\chi^2$  is performed over a finite range of  $R$ . For multiple-data-set fits, the sum for  $\chi^2$  is extended to include a sum over data sets in addition to the sum of data points for individual spectra. Modifications to the low- $R$  components of  $\chi(k)$  can be made using the *AUTOBK* (Newville *et al.*, 1993) algorithm. Though rarely altering the fit results, this allows correlations between background and structural variables to be assessed.

Estimates for  $\delta\mathbf{x}$ , the uncertainties of the fitted variables  $\mathbf{x}$ , and  $\mathbf{C}(\mathbf{x}_i, \mathbf{x}_j)$ , the correlations between variable pairs, are made at the 'best fit' condition ( $\mathbf{x} = \mathbf{x}_0$ ), according to the standard statistical treatment of experimental data (Bevington, 1969). Because the estimate of the uncertainty of the data is not always reliable, the uncertainties estimated this way are rescaled by  $\chi^2/\nu^{1/2}$  where  $\nu = N_{\text{info}} - P$ . Both  $\chi^2$  and  $\chi^2/\nu$  are reported, as is an EXAFS  $\mathcal{R}$  factor that gives the misfit relative to the data size.

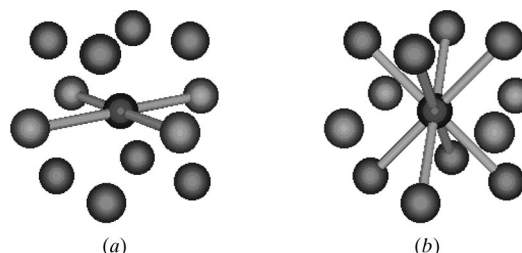


**Figure 2** In-plane (a) and out-of-plane (b) scattering paths for  $\text{CoPt}_3$ . In the ordered structure, Co is completely surrounded by Pt, as shown.

**Table 2**

 Summary of fit results for Co *K*-edge EXAFS of CoPt<sub>3</sub> grown with a substrate temperature of 723 K.

Variable	Best-fit value	(uncertainty)
$\alpha$	0.48	(0.10)
$\beta$	0.12	(0.09)
$R_{\text{Pt}}$	2.691	(0.004)
$R_{\text{Co}}$	2.671	(0.008)
$\sigma_{\text{Pt}}^2$	0.007	(0.001)
$\sigma_{\text{Co}}^2$	0.009	(0.002)
$N_{\parallel}$	3.35	(0.20)
$N_{\perp}$	7.87	(0.33)
$E_0$	2.04	(0.23)

#### 4. Example: anisotropy in CoPt<sub>3</sub>: Co *K* edge

As an example, we study the anisotropy in the Co and Pt distribution in CoPt<sub>3</sub> films, grown along the (100) direction (Cross *et al.*, 2001). Without addressing too many of the material science points of interest (Rooney *et al.*, 1995; Shapiro *et al.*, 1996; Meneghini *et al.*, 1999; Tyson *et al.*, 1996), the goal for the EXAFS analysis is to investigate any difference in Co–Co pairing in and out of the growth plane. In a fully disordered state, CoPt<sub>3</sub> assumes an f.c.c. lattice, with random population of Co and Pt. A fully ordered L1<sub>2</sub> structure (similar to the ordered Cu<sub>3</sub>Au phase) is an f.c.c. lattice with Co on cube corners and Pt on cube faces.

Polarized EXAFS measurements were made at Advanced Photon Source sector 20 (PNC-CAT) at both the Co *K* edge and Pt *L*<sub>III</sub> edges for a set of four samples (each with different substrate temperatures during deposition), with the polarization vector of the incident X-rays perpendicular to and parallel to (within 5°) the (100) plane (Cross *et al.*, 2001). Because of the simple cos<sup>2</sup> dependence of the *K*-edge polarization (as opposed to the somewhat more complicated

*L*<sub>III</sub>-edge polarization), unpolarized *FEFF* calculations were performed for the Co edge, and the polarization dependence will be included explicitly with *FEFFIT*. This allows one *feffnnn.dat* file to be used for near-neighbor Co and one for near-neighbor Pt, simplifying the problem somewhat. Unpolarized *FEFF7* calculations were used.

Starting from the L1<sub>2</sub> structure, we define  $\alpha$  as the fraction of Co in-plane near neighbors, and  $\beta$  as the fraction of Co out-of-plane near neighbors. For each of the four in-plane neighbors (Fig. 2*a*), and for the eight out-of-plane neighbors (Fig. 2*b*), we have

$$\chi_{\text{IP}} = \alpha\chi_{\text{Co}} + (1 - \alpha)\chi_{\text{Pt}}, \quad (6)$$

$$\chi_{\text{NP}} = \beta\chi_{\text{Co}} + (1 - \beta)\chi_{\text{Pt}}, \quad (7)$$

and the total first-shell EXAFS for the two different polarizations (explicitly including the polarization dependence) is simply

$$\begin{aligned} \chi_{\parallel} &= (3N_{\parallel}/2)[\alpha\chi_{\text{Co}} + (1 - \alpha)\chi_{\text{Pt}}] + 3N_{\perp}[\beta\chi_{\text{Co}} + (1 - \beta)\chi_{\text{Pt}}], \\ \chi_{\perp} &= (3N_{\perp}/2)[\beta\chi_{\text{Co}} + (1 - \beta)\chi_{\text{Pt}}]. \end{aligned} \quad (8)$$

Data for both polarizations were fit simultaneously, using two paths ( $\chi_{\text{Co}}$  and  $\chi_{\text{Pt}}$ ) for each polarization. This constrains  $\alpha$  and  $\beta$  to be self-consistent. The overall amplitude factor was set as the product of  $S_0^2$  and the coefficients in equation (8). The following variables were used in the fits:  $E_0$  [one used for both data sets after carefully checking the alignment of the starting  $\mu(E)$  spectra],  $R_{\text{Pt}}$ ,  $R_{\text{Co}}$ ,  $\sigma_{\text{Pt}}^2$ ,  $\sigma_{\text{Co}}^2$ ,  $\alpha$  and  $\beta$ .  $S_0^2$  itself was fixed at 0.74 by asserting that the total number of neighbors for the sample grown at 1073 K (which is expected to be well annealed and fully disordered) was 12. Though *FEFF* does account for many loss terms in the EXAFS, this is a fairly typical value for  $S_0^2$ , and may include systematic errors in normal-

```

guess a_x = 0.25  %% Co -> in-plane Pt
guess b_x = 0.25  %% Co -> out-of-plane Pt
set a = abs(a_x) %% force these to both
set b = abs(b_x) %% be positive

guess n_out = 8.0  %% N out-of-plane
guess n_in = 4.0  %% N in-plane

%% explicit polarization dependence: (simple here!!)
set cos2 = 0.5
set ne_in = n_in * cos2
set ne_out = n_out * cos2

%% effective number of CoCo and CoPt neighbors (in-plane)
set CoCo_para= 3 * (ne_in * a + ne_out * cos2 * b)
set CoPt_para= 3 * (ne_in * (1 - a) + ne_out * cos2 * (1 - b))

%% effective number of CoCo and CoPt neighbors (out-plane)
set CoCo_perp= 3 * ne_out * b
set CoPt_perp= 3 * ne_out * (1 - b)

%% total number of Co and Pt bonds
set n_Co = n_out * b + n_in * a
set n_Pt = n_out * (1 - b) + n_in * (1 - a)

set s02 = 0.74  %% overall amplitude

%%-- FOR IN_PLANE DATA
path 1 ../feff/feff_CoCo.0001
s02 1 s02_co * CoCo_para

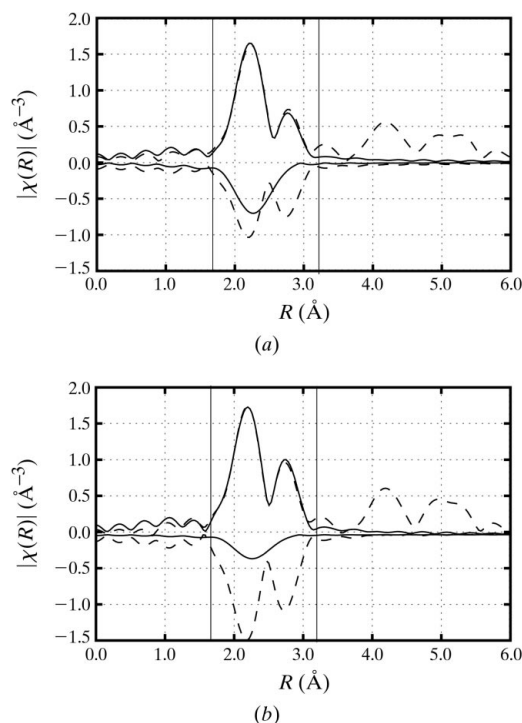
path 2 ../feff/feff_CoPt.0001
s02 2 s02_co * CoPt_para

%%-- FOR OUT_OF_PLANE DATA
path 1 ../feff/feff_CoCo.0001
s02 1 s02_co * CoCo_perp

path 2 ../feff/feff_CoPt.0001
s02 2 s02_co * CoPt_perp
    
```

**Figure 3**

Portion of *feffit.inp* setting up the fitting model for the Co *K*-edge of CoPt<sub>3</sub> described in equation (8). The fitting model is dominated by the calculation of the amplitude parameters for the in-plane and out-of-plane Co–Co and Co–Pt contributions.  $a$  represents  $\alpha$  and  $b$  represents  $\beta$ . Note that the polarization dependence here is particularly easy as the f.c.c. structure fixes all angles to be  $\pi/4$  or  $\pi/2$ .


**Figure 4**

Data (dashed) and first-shell fit (solid) of in-plane (*a*) and out-of-plane (*b*) Co EXAFS for a sample grown with a substrate temperature of 723 K. The fit  $R$ -ranges are indicated by vertical bars and the contributions from the Co and Pt neighbors are shown inverted. The Fourier transforms were performed on  $\chi(k)$  data with  $k_{\text{min}} = 1.0 \text{ \AA}^{-1}$ ,  $k_{\text{max}} = 10.0 \text{ \AA}^{-1}$ ,  $dk = 0.3 \text{ \AA}^{-1}$  for Hanning windows, and  $k$ -weight = 2.

ization as well as an incomplete accounting of the loss terms. The total numbers of in-plane neighbors  $N_{\parallel}$  and out-of-plane neighbors  $N_{\perp}$  were also varied in the fit.

Fig. 3 shows a portion of the *feffit.inp* file setting up this model, including the polarization dependence. The fit results for the CoPt<sub>3</sub> sample grown at a substrate temperature of 723 K are shown in Table 2, and the final fit of  $\chi(R)$  is shown in Fig. 4. The values for the best-fit statistics were  $\chi^2 = 392$ ,  $\chi_v^2 = 39$  and  $\mathcal{R} = 0.003$ .

## 5. Conclusions

The use of *FEFF* and *FEFFIT* has been described and demonstrated for a simultaneous fit of two polarizations of Co *K*-edge EXAFS of CoPt<sub>3</sub>. *FEFFIT* adds robust data modeling and fitting capabilities to *FEFF* while retaining a high level of precision. Despite the wide use of both *FEFF* and *FEFFIT*, there has been little formal training for using these programs, and little effort to make them accessible to novices. A recent series of workshops (Ravel, 2000), this paper, and the recently released *IFEFFIT* program (Newville, 2001) are attempts to overcome these shortcomings.

I thank John Rehr, Edward Stern, Bruce Ravel, Steve Zabinsky, Alex Ankudinov and Julie Cross for helpful discussions. Many users of *FEFFIT* have helped to make it more robust and useful, especially Anatoly Frenkel, Boyan Boyanov, Chuck Bouldin, Daniel Haskel and Shelly Kelly. Thanks to Vince Harris and Julie Cross for the data used as the example in this paper.

## References

- Ankudinov, A. L., Conradson, S. D., de Leon, J. M. & Rehr, J. J. (1998). *Phys. Rev. B*, **57**, 7518–7565.
- Ankudinov, A. L., Ravel, B., Rehr, J. J. & Conradson, S. D. (1998). *Phys. Rev. B*, **57**, 7565–7576.
- Ankudinov, A. L. & Rehr, J. J. (1995). *Phys. Rev. B*, **51**(2), 1282–1285.
- Ankudinov, A. L. & Rehr, J. J. (1997). *Phys. Rev. B*, **56**, R1712–R1715.
- Bevington, P. R. (1969). *Data Reduction and Error Analysis for the Physical Sciences*. New York: McGraw-Hill.
- Binsted, N., Campbell, J. W., Gurman, S. J. & Stephenson, P. C. (1991). *SERC Daresbury Laboratory Report*. Daresbury Laboratory, Daresbury, Warrington WA4 4AD, UK.
- Binsted, N. & Hasnain, S. S. (1996). *J. Synchrotron Rad.* **3**, 185–196.
- Binsted, N., Strange, R. W. & Hasnain, S. S. (1992). *Biochemistry*, **31**, 12117–12125.
- Bouldin, C. E., Elam, W. T. & Furenlid, L. (1995). *Physica B*, **208/209**, 190–192.
- Bridges, F. & Rehr, J. J. (1998). Personal communication.
- Brillouin, L. (1962). *Science and Information Theory*. New York: Academic Press.
- Bunker, G. (1983). *Nucl. Instrum. Methods*, **207**, 437–444.
- Cross, J. O., Newville, M., Hellman, F., Rooney, P. W., Shapiro, A. L. & Harris, V. G. (2001). *J. Synchrotron Rad.* **8**, 880–882.
- Curis, E. & Benazeth, S. (2000). *J. Synchrotron Rad.* **7**, 262–266.
- Filippini, A., Cicco, A. D. & Natoli, C. R. (1995). *Phys. Rev. B*, **52**, 15122–15134.
- Frenkel, A., Stern, E. A., Voronel, A., Qian, M. & Newville, M. (1994). *Phys. Rev. B*, **49**(17), 11662–11674.
- Frenkel, A., Vairavamurthy, M. & Newville, M. (2001). *J. Synchrotron Rad.* **8**, 669–671.
- George, G. N. & Pickering, I. J. (1995). *EXAFS-PAK*. Technical Report. Stanford Synchrotron Radiation Laboratory, Stanford, CA, USA.
- Hasnain, S. S., Helliwell, J. R. & Kamitsubo, H. (1999). *J. Synchrotron Rad.* **6**, 121–122.
- Kelly, S., Ingalls, R., Wang, F., Ravel, B. & Haskel, D. (1998). *Phys. Rev. B*, **57**(13), 7543–7550.
- Kendall, M. G. (1958). *The Advanced Theory of Statistics*, Vol. 1. London: Charles Griffin.
- Krappe, H. J. & Rossner, H. H. (2000). *Phys. Rev. B*, **61**(10), 6596–6610.
- Lytle, F. W., Sayers, D. E. & Stern, E. A. (1989). *Physica B*, **158**, 701–722.
- Marquardt, D. W. (1963). *J. Soc. Ind. Appl. Math.* **11**, 431–441.
- McKale, A. G., Veal, B. W., Paulikas, A. P., Chan, S. L. & Knapp, G. S. (1988). *J. Am. Chem. Soc.* **110**, 3763–3768.
- Meneghini, C., Maret, M., Parasote, V., Cadeville, M. C., Hazemann, J. L., Cortes, R. & Colonna, S. (1999). *Eur. Phys. J. B*, **7**, 347–357.
- Michalowicz, A. (1995). *Physica B*, **208/209**, 190–192.
- Newville, M. (2001). *J. Synchrotron Rad.* **8**, 322–324.
- Newville, M., Boyanov, B. & Sayers, D. E. (1999). *J. Synchrotron Rad.* **6**, 264–265.
- Newville, M., Livins, P., Yacoby, Y., Rehr, J. J. & Stern, E. A. (1993). *Phys. Rev. B*, **47**(21), 14126–14131.
- Newville, M., Ravel, B., Haskel, D., Rehr, J. J., Stern, E. A. & Yacoby, Y. (1995). *Physica B*, **208/209**, 154–156.
- O'Day, P. A., Rehr, J. J., Zabinsky, S. I. & Brown, G. (1994). *J. Am. Chem. Soc.* **116**(7), 2938–2949.
- Ravel, B. (2000). *EXAFS Analysis Using FEFF and FEFFIT*. A workshop with course materials available on CD-ROM at <http://feff.Phys.washington.edu/ravel/course/>.
- Ravel, B. (2001). *J. Synchrotron Rad.* **8**, 314–316.
- Ravel, B., Cockayne, E., Newville, M. & Rabe, K. M. (1999). *Phys. Rev. B*, **60**(21), 14632–14642.
- Rehr, J. J. & Albers, R. C. (1990). *Phys. Rev. B*, **41**(12), 8139–8149.
- Rehr, J. J. & Albers, R. C. (2000). *Rev. Mod. Phys.* **72**, 621–654.
- Rehr, J. J., Albers, R. C., Natoli, C. R. & Stern, E. A. (1986). *Phys. Rev. B*, **34**, 4350.
- Rehr, J. J., Albers, R. C. & Zabinsky, S. I. (1992). *Phys. Rev. Lett.* **69**(23), 3397–3400.
- Rehr, J. J. & Ankudinov, A. L. (2001). *J. Synchrotron Rad.* **8**, 61–65.
- Rehr, J. J., Mustre de Leon, J., Zabinsky, S. I. & Albers, R. C. (1991). *J. Am. Chem. Soc.* **113**(14), 5135–5140.
- Ressler, T. (1997). *J. Phys. IV*, **D7**(C2), 269.
- Rooney, P. W., Shapiro, A. L., Tran, M. Q. & Hellman, F. (1995). *Phys. Rev. Lett.* **75**, 1843.
- Shapiro, A. L., Rooney, P. W., Tran, M. Q., Hellman, F., Ring, K. M. & Kavanagh, K. L. (1996). *Phys. Rev. B*, **60**, R3702.
- Stern, E. A. (1988). *X-ray Absorption: Principles, Applications, Techniques of EXAFS, SEXAFS and XANES*, edited by D. C. Koningsberger & R. Prins, Vol. 92 of *Chemical Analysis*, p. 1. New York: John Wiley.
- Stern, E. A. (1993). *Phys. Rev. B*, **48**(13), 9825–9827.
- Tranquada, J. M. & Ingalls, R. (1983). *Phys. Rev. B*, **28**(6), 3520–3528.
- Tyson, T., Conradson, S. D., Farrow, R. F. C. & Jones, B. A. (1996). *Phys. Rev. B*, **54**, R3702.
- Vaarkamp, M. (1993). PhD thesis, Technische Universiteit Eindhoven, The Netherlands.
- Vaarkamp, M., Dring, I., Oldman, R. J., Stern, E. A. & Koningsberger, D. C. (1994). *Phys. Rev. B*, **50**(11), 7872–7883.
- Zabinsky, S. I., Rehr, J. J., Ankudinov, A., Albers, R. C. & Eller, M. J. (1995). *Phys. Rev. B*, **52**(4), 2995–3009.